

## Irregular-regular mode oscillations inside plasma bubble and its fractal analysis in glow discharge magnetized plasma

Mariammal Megalingam, N. Hari Prakash, Infant Solomon, Arun Sarma, and Bornali Sarma

Citation: *Physics of Plasmas* **24**, 042304 (2017); doi: 10.1063/1.4979891

View online: <http://dx.doi.org/10.1063/1.4979891>

View Table of Contents: <http://aip.scitation.org/toc/php/24/4>

Published by the *American Institute of Physics*

---

---



Small Conferences. BIG Ideas.

Applied Physics  
Reviews

SAVE THE DATE!  
**3D Bioprinting: Physical and Chemical Processes**  
May 2–3, 2017 • Winston Salem, NC, USA

## Irregular-regular mode oscillations inside plasma bubble and its fractal analysis in glow discharge magnetized plasma

Mariammal Megalingam, N. Hari Prakash, Infant Solomon, Arun Sarma, and Bornali Sarma  
*Division of Physics, VIT University, Vandalur–Kelambakkam Road, Chennai 600127, Tamilnadu, India*

(Received 13 September 2016; accepted 21 March 2017; published online 17 April 2017)

Experimental evidence of different kinds of oscillations in floating potential fluctuations of glow discharge magnetized plasma is being reported. A spherical gridded cage is inserted into the ambient plasma volume for creating plasma bubbles. Plasma is produced between a spherical mesh grid and chamber. The spherical mesh grid of 80% optical transparency is connected to the positive terminal of power supply and considered as anode. Two Langmuir probes are kept in the ambient plasma to measure the floating potential fluctuations in different positions within the system, viz., inside and outside the spherical mesh grid. At certain conditions of discharge voltage ( $V_d$ ) and magnetic field, irregular to regular mode appears, and it shows chronological changes with respect to magnetic field. Further various nonlinear analyses such as Recurrence Plot, Hurst exponent, and Lyapunov exponent have been carried out to investigate the dynamics of oscillation at a range of discharge voltages and external magnetic fields. Determinism, entropy, and  $L_{max}$  are important measures of Recurrence Quantification Analysis which indicate an irregular to regular transition in the dynamics of the fluctuations. Furthermore, behavior of the plasma oscillation is characterized by the technique called multifractal detrended fluctuation analysis to explore the nature of the fluctuations. It reveals that it has a multifractal nature and behaves as a long range correlated process. *Published by AIP Publishing.* [<http://dx.doi.org/10.1063/1.4979891>]

### I. INTRODUCTION

Periodic and chaotic phenomena are commonly observed in laboratory plasmas. Various behaviors like self-oscillation, period doubling, bifurcation, intermittency, quasi-periodicity, and chaos have been studied in laboratory plasma.<sup>1</sup> In an undriven plasma system, deterministic chaos has been experimentally observed by Qin *et al.*<sup>2</sup> It shows the two routes to chaos: through period-doubling and intermittent chaos. Furthermore, DC glow discharge plasma is not driven by any external periodic force to exhibit the self-generated oscillation whose frequency varies with the control parameters of discharge.

A new diagnostic tool called as Recurrence Plot (RP) has been introduced by Eckmann *et al.*<sup>3</sup> for the study of complex behavior of the diagnostic system. RPs are, in fact, graphical, two dimensional representations showing the instants of time at which a phase space trajectory returns approximately to the same regions of phase space and can be quantified by recurrence based diagnostics like determinism (DET), Shannon, laminarity, trapping time, etc.<sup>4</sup>

Recurrence quantification analysis (RQA) techniques are being used to investigate the turbulence and its associated cross field transport in fusion plasmas.<sup>5</sup> RQA has been worked out in floating potential fluctuations (FPF) of the glow discharge unmagnetized plasma, to comprehend the dynamics of the system and, in addition, to identify the underlying physics when a system shows a transition due to changes in the controlling parameter.<sup>6</sup> Investigation of coherent modes using chaotic time series has been done<sup>7</sup> by comparing empirical mode decomposition and discrete wavelet transform. Nonlinear analyses such as time series,

power spectrum analysis, and correlation coefficient have also been espoused.

With regard to laboratory plasma, we often observe a regular, irregular, complex, and multiscale nature of the fluctuations. Hence, fluctuations are highly representing a dynamical system, and it has been subjected by many factors such as pressure, types of gases used, noises, and external field. When an external magnetic field is applied, the dynamics of the system become more complex owing to the generation of various magnetized plasma modes like  $E \times B$  drift, cyclotron modes, etc. This fluctuation demonstrates chaotic nature but with self-similar behavior and also evidences for strong fluctuations of all probable scales.<sup>8</sup> Therefore, the dynamical change in plasma fluctuations needs to understand and investigate to evolve its physical properties.<sup>9</sup> Unique fluctuations are commonly affected due to the restrictions of the experimental setup for measuring the fluctuations. Hence, to study the original fluctuations and elude spurious finding of correlations, one has to think of using a vigorous method which should be insensitive to any nature of the fluctuations. Therefore, an attempt has been made to understand the complex behavior and multifractal dynamics of FPF obtained from the glow discharge magnetized plasma device in various experimental conditions using a technique, viz., multifractal detrended fluctuation analysis (MF-DFA).<sup>10</sup>

Kimiagar *et al.*<sup>9</sup> has used MF-DFA to study the plasma electrical discharge current fluctuations to examine its multifractal properties. MF-DFA results for original time series are compared with shuffled and surrogate series which illustrate that correlation of the fluctuations is responsible for the multifractal nature. Space plasmas have been studied using the concept of multifractality<sup>11</sup> because it allows us to look at the

intermittent turbulence in the solar wind.<sup>12</sup> Multifractality and intermittency levels are found in the tokamak plasma edge turbulence measurements comparable to the levels measured in neutral fluid turbulence done by Carreras *et al.*<sup>13</sup>

In this study, an effort has been made to instigate MF-DFA and recurrence quantification analysis (RQA) to investigate the nonlinear dynamics of the glow discharge plasma oscillations in the presence of an external magnetic field. The circumference of the spherical mesh grid has been considered to form plasma bubbles by developing the density gradient. Several studies on oscillating plasma bubbles have been done by Stenzel and Urrutia<sup>14</sup> by introducing mesh grid. Observations on irregular to regular oscillation through relaxation oscillation in both inside and outside oscillating plasma bubbles and its analysis have been carried out in magnetized glow discharge plasma. Visual changes in RPs are a good approach to detect the transition in FPF. RQA quantification variables have been taken into account to study about the transitions in the dynamics. The investigation of long range correlation of the FPF has been executed by using MF-DFA, which estimates the multiple exponents of plasma oscillations in the presence of different trends and also leads to study the multifractal nature of the fluctuations.<sup>9</sup>

The paper is organized as follows. Sec. II shows the analysis techniques and its relevant theory; Sec. III describes the experimental setup while Sec. IV contains the results and nonlinear analysis of the same, and finally, the conclusions of the report are presented in Sec. V.

## II. ANALYSIS TECHNIQUES AND ITS THEORY

### A. Recurrence plot

RP analysis of nonlinear time series is a relatively new and advanced technique introduced by Eckmann *et al.*<sup>4</sup> RP provides clear information about the time evaluation of phase space trajectory. The details are reported elsewhere.<sup>6</sup>

### B. Recurrence quantification variables

Using the several statistical measures, we can quantify the characteristics of the different structures appearing in a RP form, a diagnostics tool known as the Recurrence Quantification Analysis (RQA). For example, the RQA measure determinism (DET) gives the ratio of the number of recurrence points in the diagonal lines to all the recurrence points. The longest diagonal line ( $line_{max}$ ) in the RP is related to the exponential divergence of phase space trajectory.<sup>15</sup> Diagonal lines of RP plots are pinpointing the time series behavior and specifying similar evolution of states at different times.<sup>16</sup> Single, isolated recurrence points can occur in the dynamical system if states are rare, if they persist only for a very short time or fluctuate robustly.

DET is the measures of predictability of the dynamical system using the diagonal lines from RP. Diagonal line segments must have a minimum length defined by the line parameter.<sup>17</sup> The name determinism comes from repeating or deterministic patterns in the dynamic, and it shows the range in which a piece of the trajectory is close to another at

a different time. Usually, periodic signals (e.g., sine waves) will give very long diagonal lines, chaotic signals (e.g., Hénon attractor) will give very short diagonal lines, and stochastic signals (e.g., random numbers) will give no diagonal lines at all. The details of DET, ENT, and Lmax are discussed elsewhere.<sup>6</sup>

### C. Multifractal detrended fluctuation analysis

Detrended fluctuation analysis (DFA) is one of the methods developed to look at the scale invariant structure of fractal nature of the real time series. Using this technique, monofractal scaling properties and its long range correlations in noisy, nonstationary time series,<sup>17</sup> geology,<sup>18</sup> etc., could be determined. It was mainly used to find out the long range persistent behavior of the physical and biological complex dynamical systems.

Generally, correlated and uncorrelated time series could have been present in the real time system. The important features have remained unexplained,<sup>19</sup> such as the mechanism of ion and electron movements and its interactions, fractals nature of the fluctuations, effects of trends in small and large scales, and the kinds of correlations. The monofractal or multifractal nature of fluctuations would exist in the system. The monofractal signals can be described using one scaling exponent. However, many time series do not exhibit a simple monofractal scaling behavior. In order to satisfy a multitude of scaling exponents, it is required to apply a multifractal analysis. Multifractality may be due to different (time) correlations for small and large fluctuations. However, the DFA is further extended to MF-DFA for establishing its multifractal scaling properties. It has been effectively applied to diverse problems such as ones relating to heart rate dynamics,<sup>20</sup> economical time series,<sup>21</sup> etc. Therefore, plasma fluctuations may reflect fractal, monofractal, and multifractal in nature, and scale invariant feature, which can be characterized by long range power law correlations. Hence, a complex behavior of plasma oscillations and its scaling properties can be characterized by the MF-DFA method.

It is based on the identification of the scaling behavior of the  $q$ th moments and is the generalization of the standard DFA, which uses only the second moment,  $q = 2$ .<sup>22,23</sup> The reason for the underlying trends in the experimental data is not known in common. For a reliable detection of the correlations, it is necessary to distinguish trends from the intrinsic fluctuations in data. This can be done by Hurst rescaled range analysis.<sup>24</sup> Therefore, MF-DFA has been used to analyze the FPF obtained with Langmuir probe to study its multifractal properties. It is a well-established method for determining the scaling behavior of noisy data in the presence of trends without knowing their origin and shape.<sup>25</sup>

The MF-DFA consists of four steps. If  $x_k$  is a series of length  $N$ , in the first step, mean of the signal  $x_k$  is subtracted from the signal, where  $i = 1, 2, \dots, N$  and  $N$  is the length of the signal. It is expressed as

$$Y(i) \equiv \sum_{k=1}^i [x_k - \langle x \rangle] \quad i = 1, 2, \dots, N, \quad (1)$$

where  $x$  stands for the mean.

The profile is then divided into  $N_s \equiv \text{int}(N/s)$  non-overlapping segments of equal lengths  $s$ , and then computing the fluctuation function for each segment

$$F^2(s, m) \equiv \frac{1}{s} \sum_{i=1}^s \{Y[(m-1)s+i] - y_m(i)\}^2, \quad (2)$$

where  $y_m(i)$  is a fitting polynomial in segment  $m$ .

Averaging the local fluctuation function over all the parts is given by

$$F_q(s) \equiv \left\{ \frac{1}{N} \sum_{m=1}^{N_s} [F^2(s, m)]^{q/2} \right\}^{1/q}. \quad (3)$$

Generally,  $q$  can take any real value, except zero. For  $q=2$ , the standard DFA procedure is retrieved. Eventually, the slope of the log-log plot of  $F_q(s)$  versus  $s$  directly resolves the so-called generalized Hurst exponent  $h(q)$

$$F_q(s) \approx s^{h(q)}, \quad (4)$$

where  $h(q)$  is the scaling exponent, named Hurst exponent ( $H$ ).

### III. EXPERIMENTAL SET UP

The experimental observations have been carried out in the DC glow discharge magnetized plasma, and the schematic diagram of the system is shown in Fig. 1. It consists of a stainless steel cylindrical chamber of 50 cm in height and 40 cm in diameter. Two mesh grids in cylindrical and spherical shapes are inserted in the chamber. The cylindrical mesh grid of 20 cm height and 20 cm diameter and the spherical mesh grid of 15 cm diameter have been considered as anode, the whole chamber is taken as cathode, and the cylindrical mesh grid is kept floating. The chamber is evacuated using a rotary pump to reach the base pressure of  $1.2 \times 10^{-2}$  mbar. A mixture of gases, i.e., Ar and  $N_2$  (of 50 SCCM), is introduced using mass flow controller at a working pressure of  $2.0 \times 10^{-1}$  mbar. An external magnetic field has been

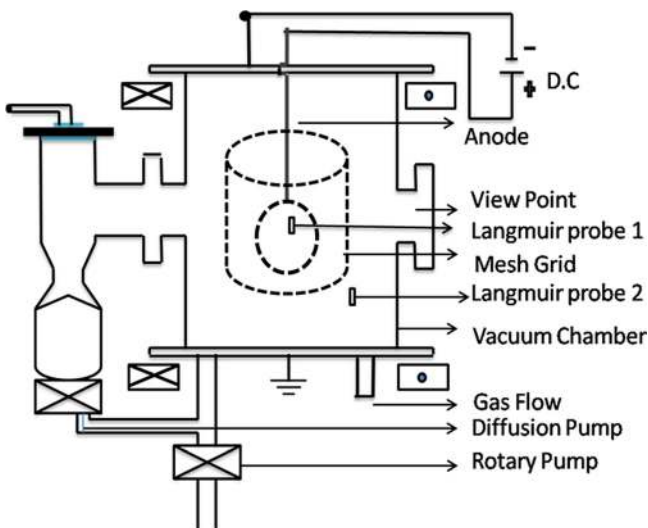


FIG. 1. Schematic diagram of the experimental setup.

provided by passing the DC current through the Helmholtz coil wound around the chamber. Langmuir probe of 2.0 mm diameter is the diagnostic tool that has been used to measure the floating potential fluctuations.<sup>26</sup> To determine the basic parameters such as plasma density and electron temperature, the current voltage (I-V) characteristic of the probe can be obtained, as the applied bias voltage  $V_B$  is swept from a negative to a positive potential. The plasma density and electron temperature are evaluated from Langmuir probe and are found to be of the order of  $10^8/\text{cc}$  and 1–3 eV. The experiment has been performed in the presence of 0–224 G magnetic field ( $B$ ) and discharge voltages. Two Langmuir probes are kept in different fixed positions to examine the dynamical transition of FPF inside the plasma bubble and near the chamber wall. Further time series corresponding to the FPF data are collected in the oscilloscope, and various nonlinear and statistical techniques have been used to evaluate their dynamical and statistical behaviours. The system shows different dynamical transitions, namely, irregular to regular mode oscillations and relaxation oscillations with changing control parameters.

### IV. RESULTS AND DISCUSSIONS

The experiment is carried out in the mixture of gases exhibiting interesting features with different magnetic fields ranging from 0 to 224 G at 300 V discharge voltages ( $V_d$ ). The magnetic field and discharge voltage are considered as controlling parameters for the whole set of experiments. The dynamics of the oscillations are sensitive on the controlling parameter, and with the variation of controlling parameter, it shows chaotic, relaxation, and periodic oscillations. At  $V_d$  is 300 V, the magnetic field is varying from 0 G to 224 G. Figs. 2 and 3 show the time series of FPF for inner Langmuir Probe (LP1) and outer Langmuir probe (LP2) that are plotted with the increase in the external magnetic fields. Fig. 2(a) shows that at 0 G magnetic field, the floating potential fluctuations are demonstrated to be chaotic in nature, which disappears completely at 42 G and becomes periodic in nature. It shows a completely periodic behavior in a relatively high magnetic field.

#### A. Floating potential fluctuations

Fig. 3 shows the oscillation observed in the outer probe, which is also shown to be chaotic in nature at a lower magnetic field. With increasing magnetic field, mixed mode oscillations are observed, i.e., large oscillations are followed by small oscillations, as shown in Fig. 3(c). It is pursuing relaxation oscillations where the large amplitudes are prominent; however, small oscillations are irregular. When  $B = 65$  G, apparent pattern of periodic fluctuations has been initiated, and it remains the same till 85 G. Figs. 3(f) and 3(g) show large and small peaks, which lead to absolute periodic in nature for the higher magnetic field  $B = 224$  G.

#### B. Power spectral analysis

The power spectral analysis of the raw data has been carried out and shown in Figs. 4 and 5. In Fig. 4, FFT clearly

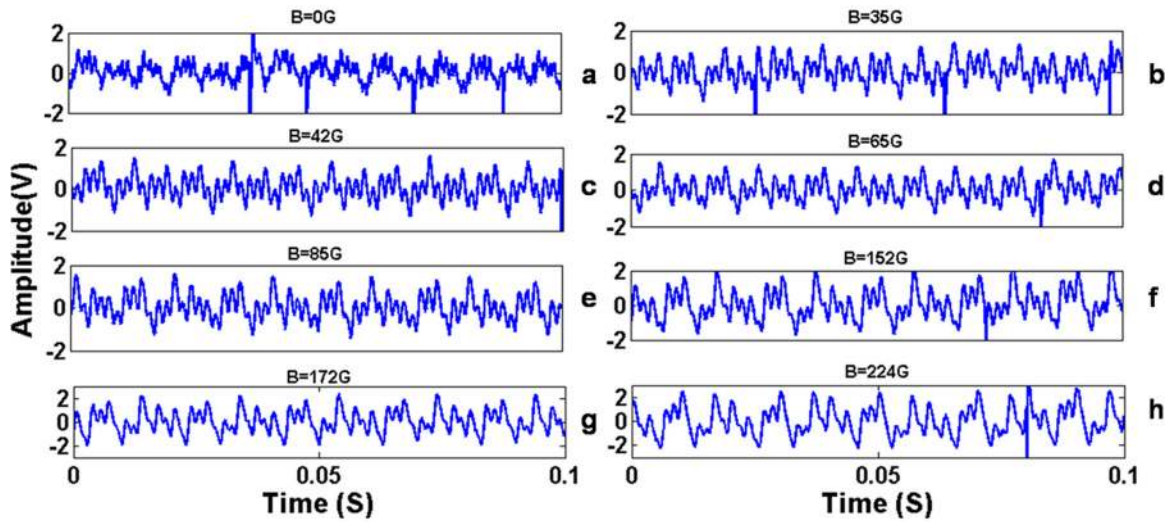


FIG. 2. Time series for FPF as a function of magnetic field measured by LP1 kept inside the spherical mesh grid at constant  $V_d = 300$  V.

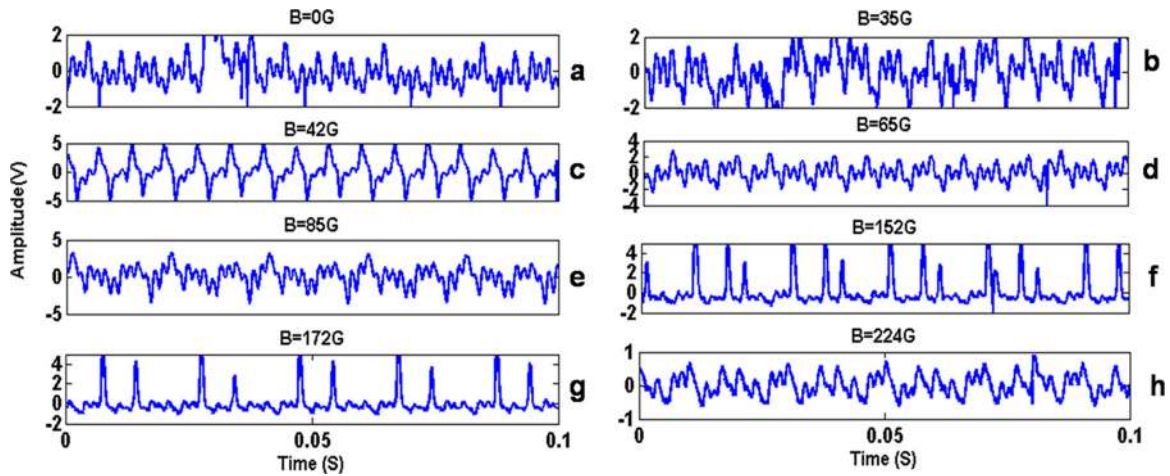


FIG. 3. Time series for FPF as a function of magnetic field measured by LP2 kept near chamber wall at  $V_d = 300$  V.

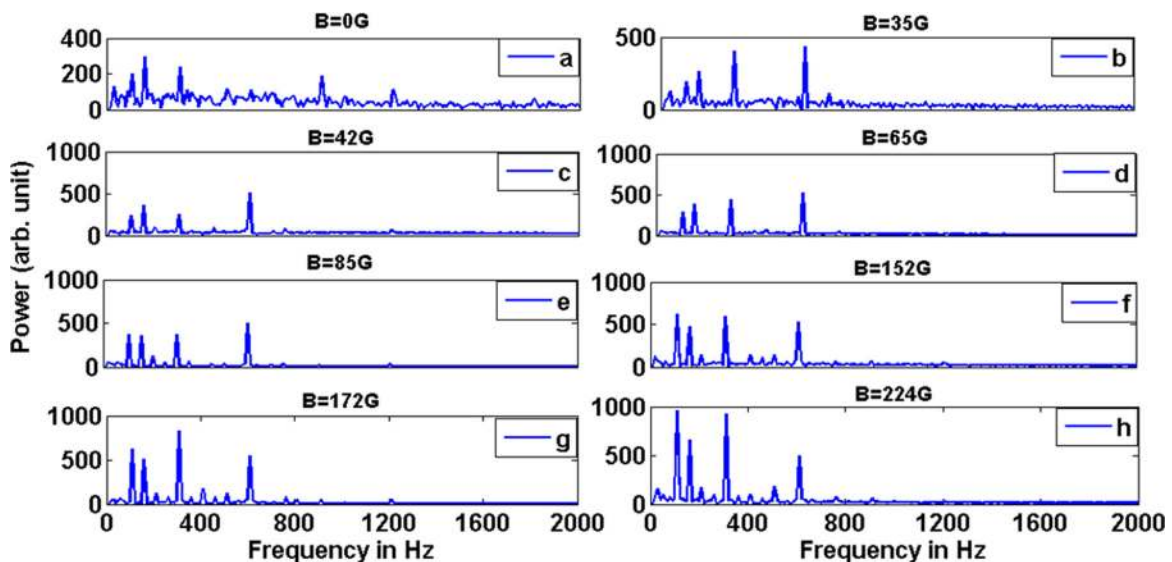


FIG. 4. Power spectra of FPF at  $V_d = 300$  V with different magnetic fields inside the spherical ball and taken by LP1.

shows a chaotic behaviour for  $B = 0$ , which also confirms the earlier analysis. Most of these frequencies are determined below 610 Hz up to  $B = 85$  G, and the dominant mode has been observed at 110 Hz when  $B = 152$  G. It has also been observed that with the increase in  $B$ , the dominant peak is shifting towards 310 Hz when the magnetic field is 172 G, and it has also been clearly noticed that amplitude elevates for the higher magnetic fields range.

In Fig. 5, the chaotic nature of floating potential fluctuations occurs at  $B = 0$  G. With the increase in  $B$ , several distinct peaks are observed ranging from 60 to 610 Hz. It clearly shows that the oscillation is relaxing from  $B = 85$  G to  $B = 172$  G. For the higher magnetic field, the system again goes to periodic nature.

### C. Phase space reconstruction

The reconstruction of the attractor gives a powerful impetus to investigate the natural phenomena in real systems. Time delays  $\tau$  are calculated from the first minimum of the average mutual information function.<sup>6</sup> It has been noticed that  $d$  and  $\tau$  for all the time series lie in the range of 4–6 and 4–30. The phase space plot (PSP) of plasma oscillations are depicted in Fig. 6 for the inner probe LP1. When  $V_d = 300$  V and  $B = 0$ , Figs. 6(a)–6(d) indicate the chaotic behavior of plasma oscillations. At  $B = 85$  G, a periodic attractor has been observed which reflects that oscillations are going towards periodic from chaotic nature with increasing magnetic field.

Fig. 7 shows the complex nature with chaotic oscillation at 300 V discharge voltage. At  $B = 85$  G, it leads to relaxation oscillations that are clearly shown in the figure. It has been noticed that it is turning to be periodic for the higher magnetic field; still, some more loops are seen due to the influence of noise.

### D. Recurrence quantification analysis

Figs. 8 and 9 show the recurrence plots of floating potential fluctuations at 300 V discharge voltages and different

magnetic fields. The data length considered for the RP is thousand points. Larger diagonal lines along with small dots as shown in Fig. 8(a) reveal that the plasma oscillations are chaotic in nature. Similar to phase space and other analyses, the chaotic nature is slowly moving toward periodic oscillations when  $B = 85$  G and shown in Fig. 8(e). The long interrupted diagonal lines interpret chaoticity of the signal. When the  $B$  is slightly increasing to 35 G, it shows interrupted diagonal lines which infer the quasi periodicity of the signal. At a higher magnetic field, the oscillations are stirring to be periodic. The distance between the diagonal lines is examined under the variation of  $B$ , which interprets the frequency of oscillation that is changing with different magnetic fields.

Fig. 9(a) represents many small diagonal lines which are discontinuous by nature. Fig. 9(b) shows long diagonal lines with small lines, indicating that oscillation has become quasi periodic, and Fig. 9(c) presents long diagonal lines that indicate the order state of oscillation. When  $B = 152$  G, the distance between the diagonal lines is large enough and also discontinuous in nature, which illustrates that the plasma oscillation is relaxed in nature. With a further increase in magnetic field, the plasma oscillation is becoming periodic in the presence of 224 G magnetic field.

Furthermore, the evolution of nonlinearity in the system with the variation in control parameters can be understood by studying some of the system properties: Lyapunov exponent (LE) and Hurst exponent. All these parameters are obtained from measurable statistical properties of the time series; as each of the statistical properties reveals different features of nonlinearity, to find out the chaoticity, periodicity, and persistence of the time series, it is important to estimate the Lyapunov exponent and Hurst exponent.

### E. Lyapunov exponent

To confirm chaoticity of a system, Lyapunov exponent (LE) needs to be calculated, and it physically defines how fast two points in phase space diverges for a time series. Let us assume  $l_0$  to be the initial separation between the two

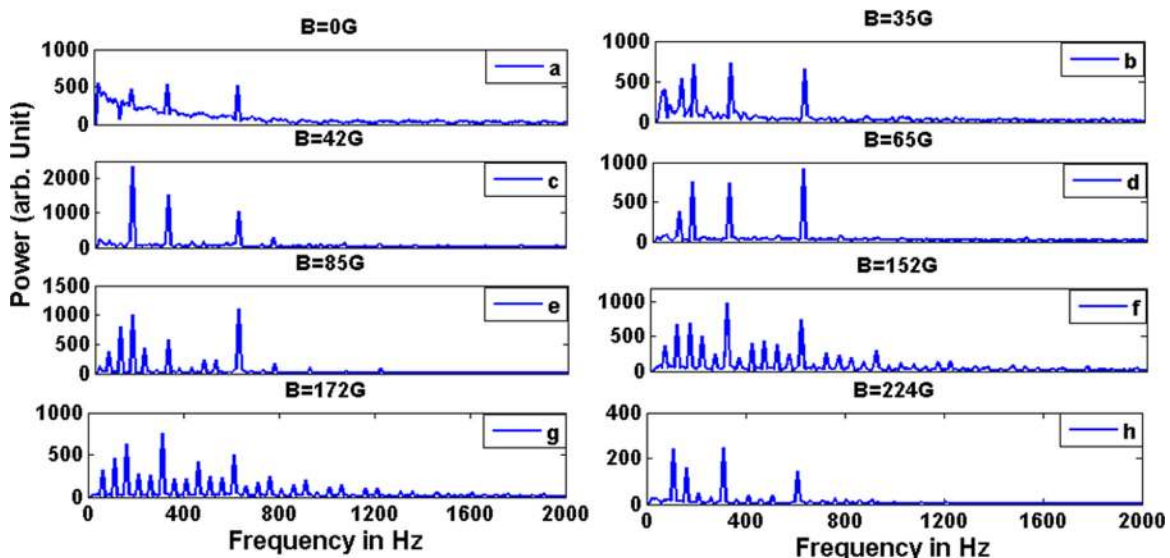


FIG. 5. Power spectra of FPF at  $V_d = 300$  V with different magnetic fields near chamber wall and taken by LP2.

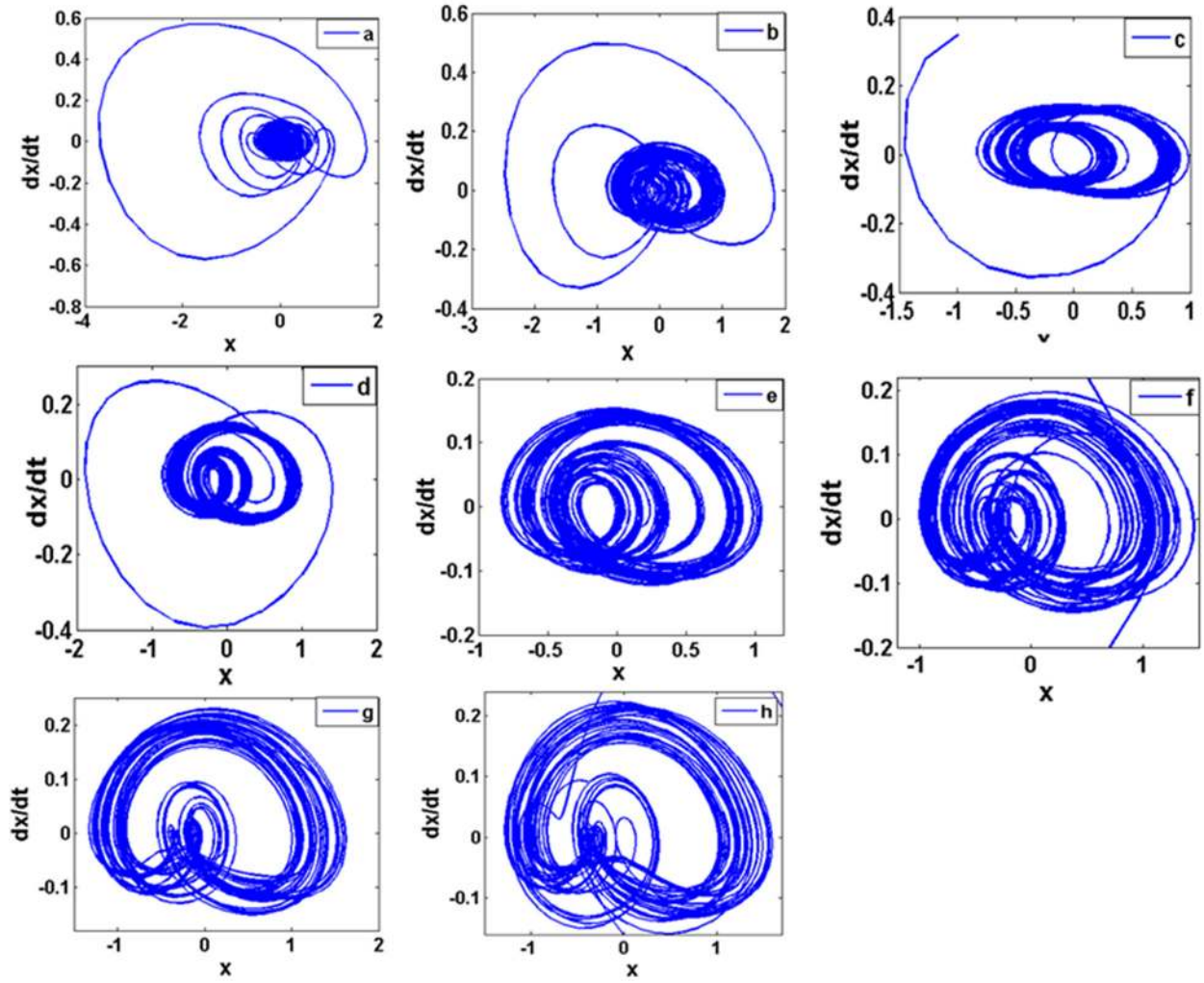


FIG. 6. The phase space plot of the FPF at different values of magnetic field: (a)  $B = 0$  G, (b)  $B = 35$  G, (c)  $B = 42$  G, (d)  $B = 65$  G, (e)  $B = 85$  G, (f)  $B = 152$  G, (g)  $B = 172$  G, and (h)  $B = 224$  G at  $V_d = 300$  V by LP1.

points in a phase space diagram. Now, if  $I(t) \sim I_0 e^{\lambda t}$ , then  $\lambda$  is the Lyapunov exponent.<sup>27</sup>

In Figure 10, we see the Lyapunov exponents for various magnetic fields. At  $B = 0$  G, the LE value is high with 0.23 and 0.18 for LP1 and LP2, and it shows the irregular behavior of the oscillations. This pattern is a clear indication that the chaoticity of the system is decreasing. With increasing  $B$ , the values of LE are gradually falling, which indicates transition. The calculated values are low and are 0.16 and 0.12. Hence, plasma as a dynamic system undergoes chaos to order for transition in this experimental condition.

Variations of recurrence quantification variables, (a) DET, (b) entropy, and (c)  $L_{max}$ , have been plotted using LP1 and LP2. Fig. 11 reflects the RQA variable at a constant discharge voltage in different magnetic fields. In this work, statistical properties of plasma oscillations have also been obtained when the external magnetic field was gradually increased from 0 to 224 G. At  $V_d = 300$  V, it has been noticed that the trend of the DET shows to be almost increasing in nature for two probes, which determines that the system is becoming more of order in higher magnetic field. The RQA variable DET resolves the periodicity of a signal. The value of DET is 1.0 for a purely periodic signal. For the experimental time

series, the corresponding periodic signal is showing the value close to 1.0 (0.99, 0.98) at  $B = 224$  G.

The variable entropy usually replicates the complexity of the system; the value of entropy is decreased with respect to the magnetic field. It explains that the value of entropy is high in the chaotic regime and low in the periodic regime.<sup>7</sup> The inverse of  $L_{max}$  is proportional to positive Lyapunov exponent.  $L_{max}$  is low in the chaotic regime and becomes high in the periodic regime.

## F. MF-DFA of plasma oscillation

Using the power law relation, the Hurst exponent ( $H$ ) is calculated between the total fluctuation functions for multiple scales. Fig. 12 reveals that the slope ( $H$ ) of the regression line is the Hurst exponent, which is calculated from the power law relation between the overall Root Mean Square (RMS). A time series has a long range correlation when  $H$  is in the interval of 0.5–1.0, it is anti correlation when  $H$  is less than 0.5 while  $H = 0.5$  replicates the short range dependent structure and random behavior.

Using the DFA technique,<sup>10</sup> Fig. 13 shows the Hurst exponent for the time series of FPF at 300 V in  $B = 224$  G

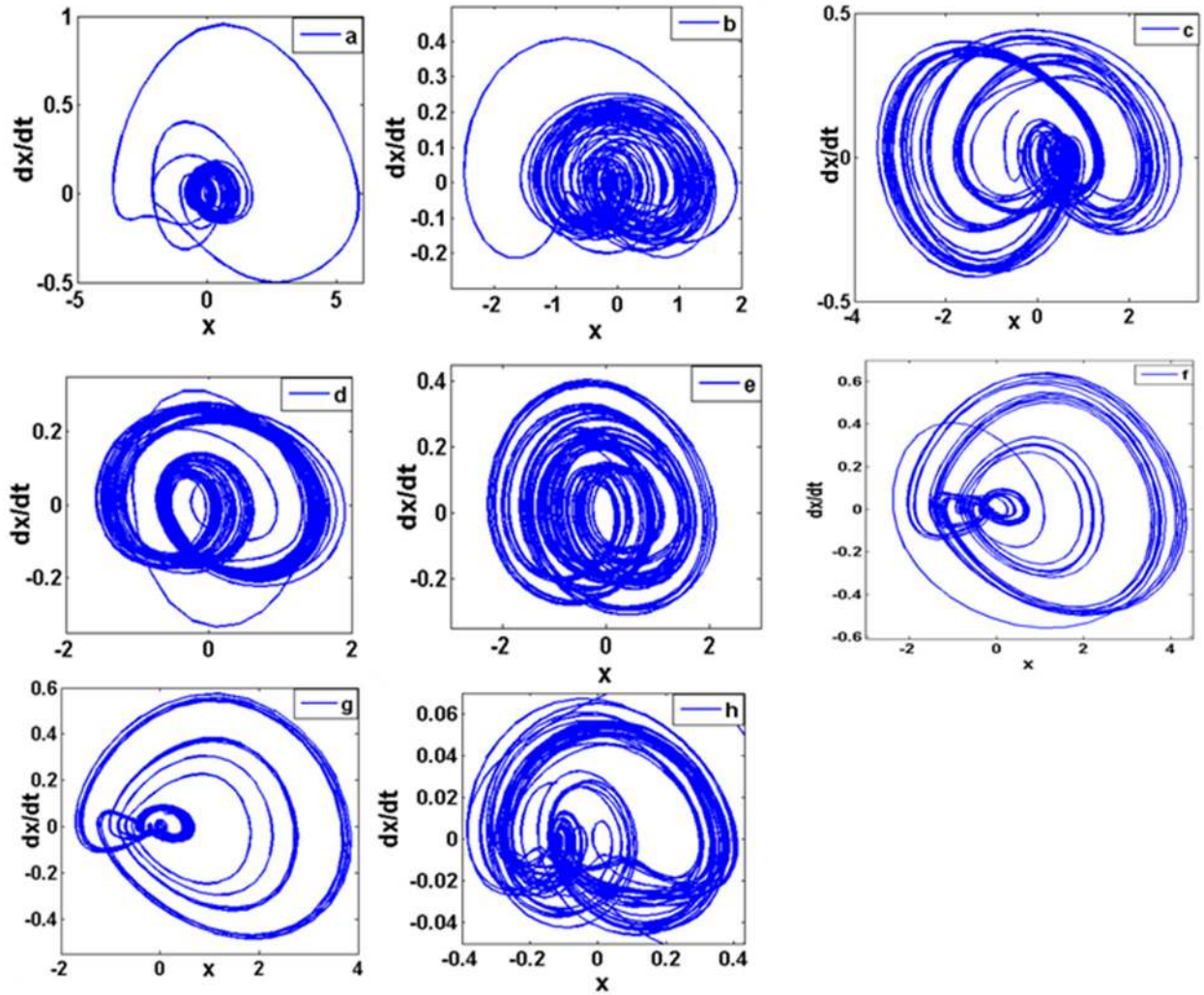


FIG. 7. The phase space plot of the FPF at different values of magnetic field: (a)  $B = 0$  G, (b)  $B = 35$  G, (c)  $B = 42$  G, (d)  $B = 65$  G, (e)  $B = 85$  G, (f)  $B = 152$  G, (g)  $B = 172$  G, and (h)  $B = 224$  G at  $V_d = 300$  V by LP2.

magnetic field. The same has been calculated for all other time series for various magnetic fields and discharge voltages. The values of the Hurst exponents of FPFs are increasing with the increase in magnetic field which indicates that a long range correlation of the floating potential fluctuation is increasing. Thus, the fluctuations are becoming regular and ordered with changing magnetic field for constant  $V_d$ . It has been observed that  $H$  is enhancing with the increase in magnetic field, and a rapid jump has been noticed at  $B = 35$  G; furthermore, it saturates with higher  $B$ . Consequently, Fig. 13 also indicates that the transitions are occurring due to increase in the magnetic field. It is clearly evident that at a lower magnetic field 36 G, the value of the  $H$  reached 0.88 and 0.91 calculated from two probes LP1 and LP2, respectively. This supposes that the correlation is less and it divulges that the plasma oscillation is irregular. Moreover, analyses like Lyapunov exponent and RQA variables also confirm that the FPF becomes periodic in higher magnetic field. Hence, the result obtained from the Hurst exponent confirms that with increasing magnetic fields, the regularity of the data increases. This is supportive of previous RQA such as DET and ENT, which is also showing the similar

trend and revealing that the system goes periodic with the increase in the magnetic field.

The time series analysis is unveiling that FPFs have many time scales. The presence of different time scales is initiated because of the simultaneous existence of plasma modes in the presence of external magnetic field. Thus, the dynamics could be studied by scaling laws, usually denoted as fractal and multifractal which are suitable for a wide range of time scales. The  $q$ -order Hurst exponent is defined as the slopes ( $H_q$ ) of regression lines (qRegline) for each  $q$ -order RMS ( $F_q$ ). It is one of the types of scaling exponents used to parameterize the multifractal structure of time series. These steps have to be followed to attain the multifractal spectrum.<sup>28</sup> The first step is to convert  $H_q$  to the  $q$ -order mass exponent ( $t_q$ ) and thereafter to convert  $t_q$  to the  $q$ -order singularity exponent ( $h_q$ ) and  $q$ -order singularity dimension ( $D_q$ ).<sup>25</sup> The plot of  $h_q$  versus  $D_q$  is referred to as the multifractal spectrum. The width and shape of the multifractal spectrum reflects the temporal variation of the local scale invariant structure of the time series, and also the width of the spectrum quantifies the degree of multifractality of a time series.

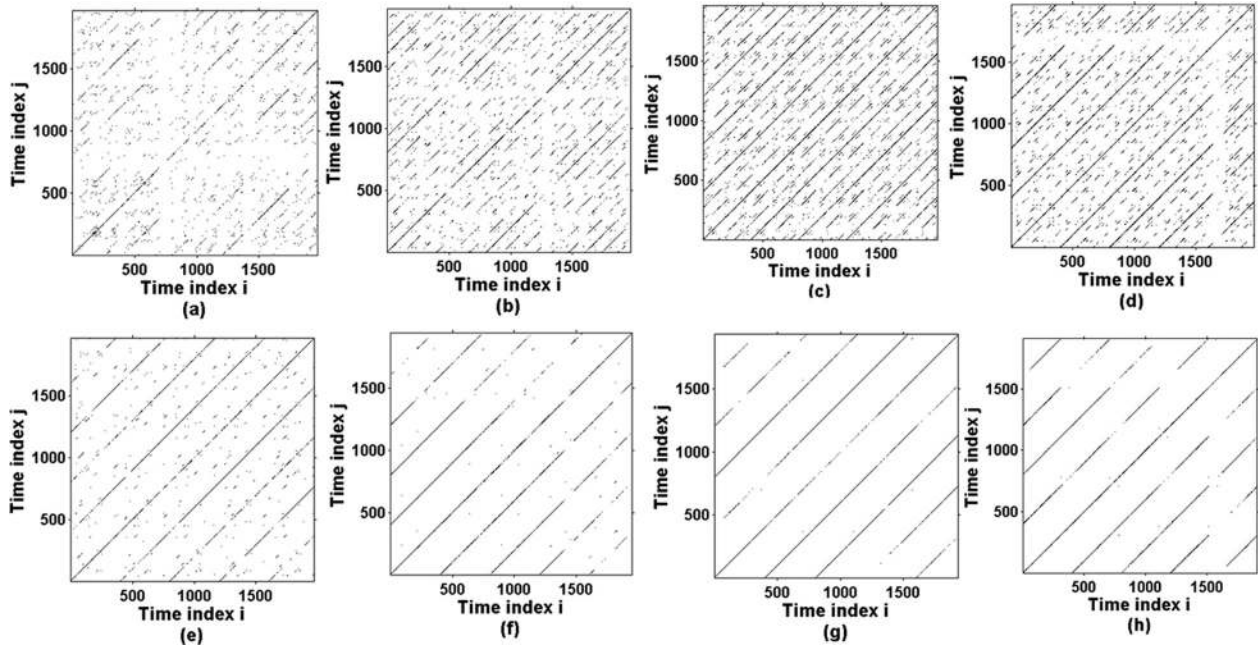


FIG. 8. Recurrence plot for FPF at different magnetic fields: (a)  $B = 0$  G, (b)  $B = 35$  G, (c)  $B = 42$  G, (d)  $B = 65$  G, (e)  $B = 85$  G, (f)  $B = 152$  G, (g)  $B = 172$  G, and (h)  $B = 224$  G at  $V_d = 300$  V by LP1.

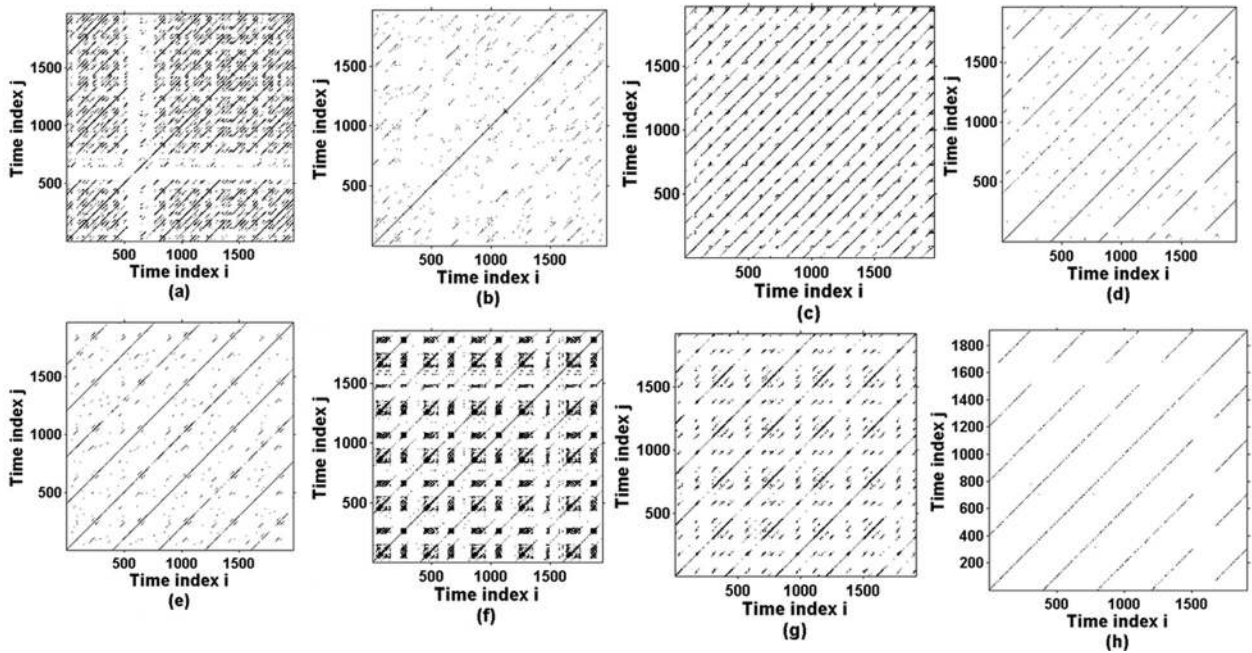


FIG. 9. Recurrence plot for FPF at different magnetic fields: (a)  $B = 0$  G, (b)  $B = 35$  G, (c)  $B = 42$  G, (d)  $B = 65$  G, (e)  $B = 85$  G, (f)  $B = 152$  G, (g)  $B = 172$  G, and (h)  $B = 224$  G at  $V_d = 300$  V by LP2.

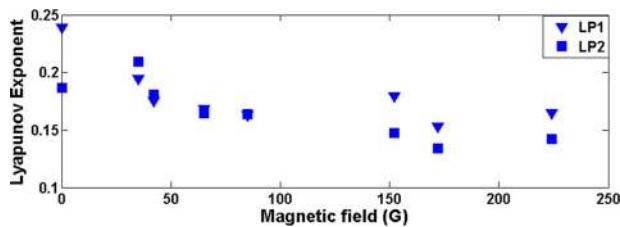


FIG. 10. Variation of Lyapunov Exponent with various magnetic fields (G) at constant  $V_d$  for LP1 and LP2.

Figs. 14(a) and 15(a) show the log-log plot of the fluctuation functions  $F_q$  vs.  $s$  for the FPF at three locations with ( $q = -5, 0, 5$ ). The difference between the  $q$ -order RMS for positive and negative  $q$ 's are visually clear at the small segment sizes compared to the large segment sizes. The fluctuation curve has different slopes, indicating different small and large fluctuation scales.

Figs. 14(b) and 15(b) reveal the growing trend of Hurst exponent  $H_q$ . When it has the negative values of  $q$ ,  $H_q$  describes the scaling behavior of segments with small

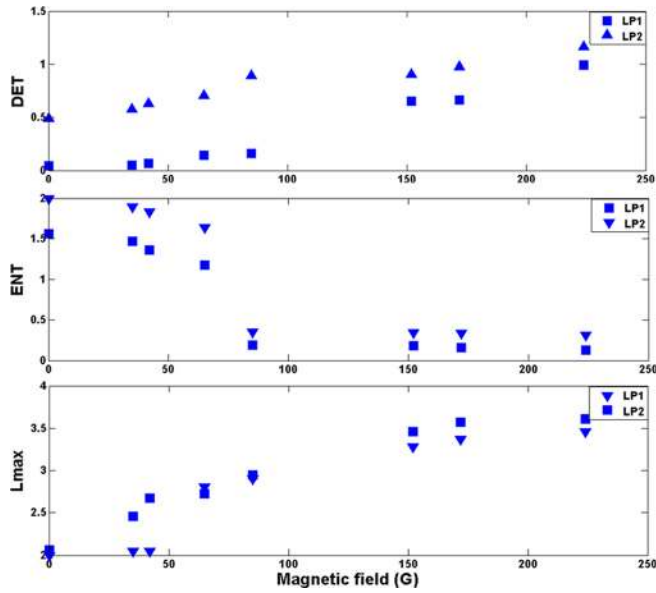


FIG. 11. Variations of recurrence quantification variables DET,  $L_{max}$ , and Entropy at constant  $V_d$  in different magnetic fields for LP1 and LP2.

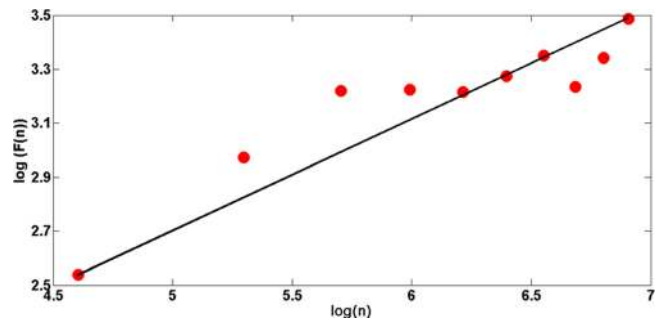


FIG. 12. Plot of  $\log(F(n))$  vs.  $\log(n)$  for time series of floating potential fluctuation at 300 V in 224 G magnetic field by LP1.

fluctuations whereas for positive values of  $q$ , it illustrates large fluctuations. One can observe from the figure that the slope has different values for various  $q$  implying that fluctuations show a multifractality nature.  $H_q$  decreases nonlinearly

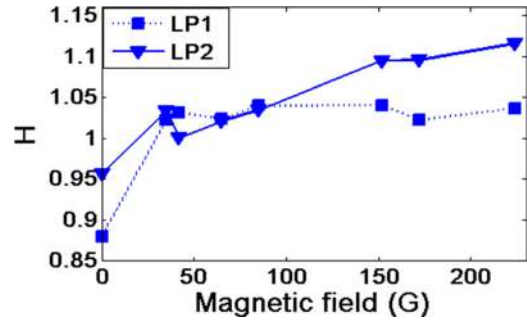


FIG. 13. Plot of Hurst exponent vs. different magnetic fields for constant  $V_d$ .

as the  $q$  value is stretching from negative to positive. Therefore, the  $H_q$  (Figure 14(b)) for the fluctuations at  $B=0$  G, the slope  $H_q$  is decreasing from 1.02 when  $q=-5$  to 0.57 when  $q=5$  as the moment  $q$  is increased from negative to positive values. Whereas in the presence of the magnetic field  $B=224$  G in Fig. 14(b), the range of  $H_q$  is reduced from 1.14 to 0.70. It is evidently pointing out the multifractal behavior<sup>29</sup> of the fluctuations and also explaining the survival of long range correlations. It also proved that  $H_q$  varies with  $q$ , which confirms that the time series is multifractal in nature, because in the case of monofractal time series which are characterized by a single exponent with over all scales, the exponent  $H_q$  is independent of  $q$ , which means there is a loss of multifractality. This dependence is considered to be a characteristic property of multifractal processes.<sup>8</sup> There is another way to perceive the multifractality behavior of the fluctuations by calculating the mass exponent  $t_q$ . The curved structure of the mass exponent  $t_q$  is dependent on the  $q$  order variable, as shown in the Figs. 14(c) and 15(c). The shape of the curve is highly nonlinear, and it shows the multifractal behavior of the fluctuations, whereas in the case of monofractal behavior, the mass exponent  $t_q$  could be of linear nature with respect to  $q$  along with a constant slope. The multifractal spectra of FPF for  $B=0$  and  $B=224$  G are shown in Figs. 14(d) and 15(d). The ensuing spectrum shows the large arc shape where the difference between the maximum and

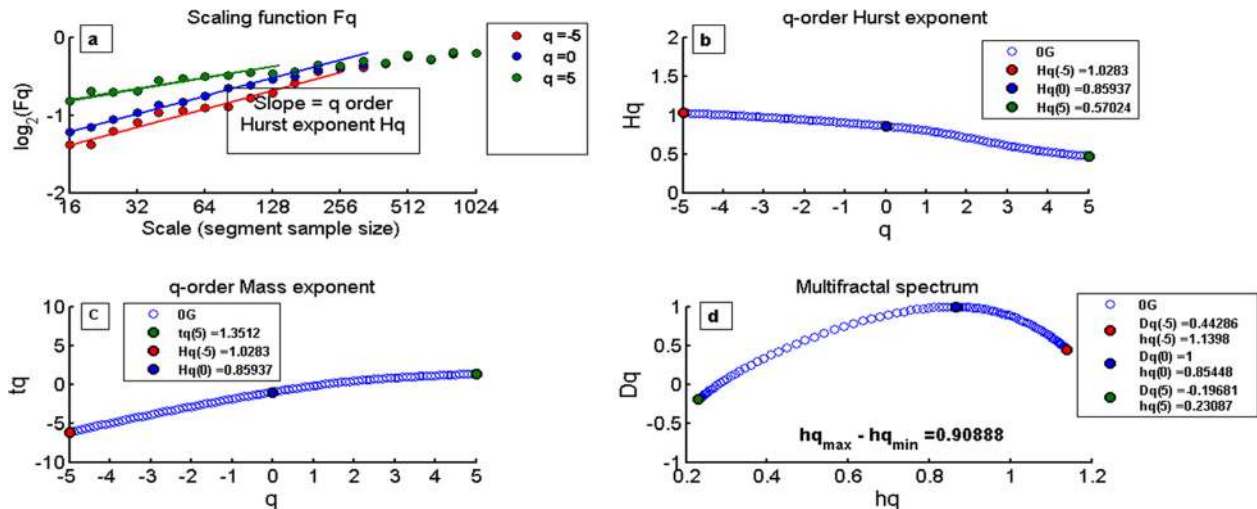


FIG. 14. Multifractal spectrum of the time series inside the spherical ball at 300 V with 0 G magnetic fields (a)  $q$ -order RMS and corresponding regression line  $q$ RegLine for multifractal time series. (b)  $q$ -order Hurst exponent  $H_q$ . (c)  $q$ -order mass exponent  $t_q$ , and (d) multifractal spectrum of  $D_q$  and  $H_q$ .

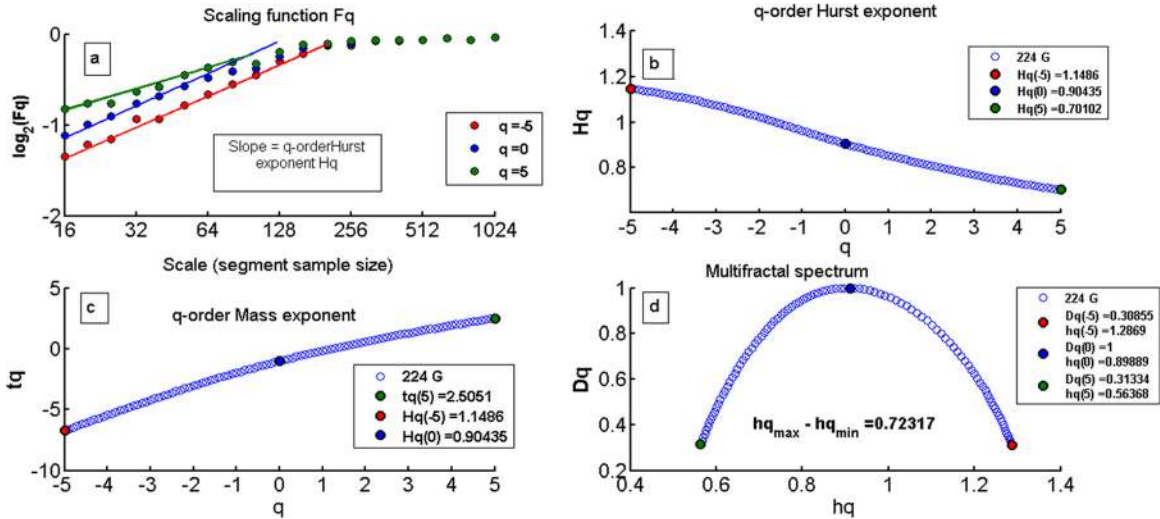


FIG. 15. Multifractal spectrum of the time series inside the spherical ball at 300 V with 224 G magnetic fields.

minimum  $h_q$  is called as the multispectrum width of the time series. The multispectrum width can also be characterized for the segments with large and small fluctuations which are deviated from the average fractal structure. We have estimated the multifractal spectrum width as 0.908 for unmagnetized fluctuations whereas the magnetized fluctuations have 0.723. It has been observed that in the presence of external magnetic field, the multifractal spectrum width decreases and the degree of multifractality also reduces. It has also been clearly understood that the multifractal nature of the time series is due to the significant existence of long range correlations.

## V. CONCLUSION

In this study, experimental investigation has been carried out to study the floating potential fluctuations influenced by oscillating plasma bubbles in a glow discharge magnetized plasma. In order to perceive the dynamical behavior of the plasma, nonlinear tools such as Power spectrum, Phase space plot, and Recurrence plot have been adopted. The plasma floating potential fluctuations are observed in the absence and presence of external magnetic field and also with discharge voltage. The recurrence based variables DET, ENT, and  $L_{\max}$  have been computed to find out the statistical behavior of the oscillations. The considered recurrence measures exhibit an immediate change, which has been confirmed in both RP plots and RQA variables. The structure of diagonal lines among all the patterns displayed in RPs clearly indicates that the irregular to regular transition is attained in the plasma oscillations associated with the magnetic field. Furthermore, a nonlinear technique such as Lyapunov exponent is reliable with previous analysis. In addition to this, the multifractal detrended fluctuation analysis (MF-DFA) has been used to identify the multifractal nature of floating potential fluctuations. It has been noticed that with the increase in magnetic field along with constant discharge voltage, the value of the Hurst exponent is increasing. Therefore, it explains that with the increase in B, long range correlation of the floating potential fluctuation is also enhancing. The effect of external magnetic field on the

multifractal property of the plasma fluctuations and their correlation has also been studied. Hurst exponent values evaluated from MF-DFA have been compared with DFA results. The values of  $H_q$  are constrained between 1.0 and 0.5 for unmagnetized and 1.1–0.7 for magnetized case, respectively. These results are the indication of the existences of long range correlations and also show the self-similar nature of the FPF. The nonlinear nature of the mass exponent  $t_q$ , the curve actively suggesting the multifractal nature of the fluctuations. It has also been observed that in the presence of external magnetic field, the multifractal spectrum width decreases and the degree of multifractality also reduces. Moreover, it can be concluded that the plasma fluctuations in this study have large and small fluctuations as seen in the power spectral analysis.

## ACKNOWLEDGMENTS

The authors would like to thank ISRO, Government of India, for providing financial support towards the research work (Grant No. ISRO/RES/2/391/2014-15).

- W. X. Ding, H. Q. She, W. Huang, and C. X. Yu, "Controlling chaos in a discharge plasma," *Phys. Rev. Lett.* **72**, 96 (1994).
- J. Qin, L. Wang, D. P. Yuan, P. Gao, and B. Z. Zhang, "Chaos and bifurcations in periodic windows observed in plasmas," *Phys. Rev. Lett.* **63**, 163 (1989).
- J.-P. Eckmann, S. O. Kamphorst, and D. Ruelle, "Recurrence plots of dynamical systems," *Europhys. Lett.* **4**, 973 (1987).
- N. Marwan, N. Wessel, U. Meyerfeldt, A. Schirdewan, and J. Kurths, "Recurrence plot based measures of complexity and its application to heart rate variability data," *Phys. Rev. E* **66**, 026702 (2002).
- N. Marwan, "A historical review of recurrence plots," *Eur. Phys. J.: Spec. Top.* **164**(1), 3–12 (2008).
- V. Mitra, A. Sarma, M. S. Janaki, A. N. S. Iyengar, B. Sarma, N. Marwan, J. Kurths, P. K. Shaw, D. Saha, and S. Ghosh, *Chaos, Solitons Fractals* **69**, 285–293 (2014).
- P. K. Shaw, D. Saha, S. Ghosh, M. S. Janaki, and A. N. S. Iyengar, *Chaos, Solitons Fractals* **78**, 285–296 (2015).
- B. A. Carreras, B. P. Van Milligen, M. A. Pedrosa, R. Balbn, C. Hidalgo, D. E. Newman, E. Sanchez, M. Frances, I. Garca-Corts, J. Bleuel, and M. Ender, "Self-similarity of the plasma edge fluctuations," *Phys. Plasmas* **5**(10), 3632 (1998).
- S. Kimiagar, M. S. Movahed, S. K. S. Sobhanian, and M. R. R. Tabar, *J. Stat. Mech.* P03020 (2009).

- <sup>10</sup>J. W. Kantelhardt, S. A. Zschiegner, E. K. Bunde, S. Havlin, A. Bunde, and H. E. Stanley, "Multifractal detrended fluctuation analysis of nonstationary time series," *Physica A* **316**(1–4), 87–114 (2002).
- <sup>11</sup>W. M. Macek, "Multifractality and intermittency in the solar wind," *Nonlinear Process. Geophys.* **14**(6), 695–700 (2007).
- <sup>12</sup>E. Marsch and C.-Y. Tu, "Intermittency, non-Gaussian statistics and fractal scaling of MHD fluctuations in the solar wind," *Nonlinear Process. Geophys.* **4**(2), 101–124 (1997).
- <sup>13</sup>B. A. Carreras, V. E. Lynch, D. E. Newman, R. Balbin, J. Bleuel, M. A. Pedrosa, M. Endler, B. van Milligen, E. Sanchez, and C. Hidalgo, *Phys. Plasmas* **7**, 3278 (2000).
- <sup>14</sup>R. L. Stenzel and J. M. Urrutia, *Phys. Plasmas* **19**, 082105 (2012).
- <sup>15</sup>N. Marwan and J. Kurths, *Phys. Lett. A* **336**, 349 (2005).
- <sup>16</sup>S. Schinkel, N. Marwan, O. Dimigen, and J. Kurths, *Phys. Lett. A* **373**, 2245 (2009).
- <sup>17</sup>B. D. Malamud and D. I. Turcotte, "Self-affine time series: Measures of weak and strong persistence," *J. Stat. Plann. Infer.* **80**(1), 173–196 (1999).
- <sup>18</sup>R. G. Kavasseri and R. Nagarajan, "A multifractal description of wind speed records," *Chaos, Solitons Fractals* **24**(1), 165–173 (2005).
- <sup>19</sup>M. V. Isupov and I. M. Ulanov, *High Temp.* **43**, 169 (2005).
- <sup>20</sup>C. K. Peng, S. Havlin, H. E. Stanley, and A. L. Goldberger, *Chaos* **5**(1), 82–87 (1995).
- <sup>21</sup>R. N. Mantegna and H. E. Stanley, *Introduction to Econophysics: Correlations and Complexity in Finance* (Cambridge University Press, Cambridge, 2000).
- <sup>22</sup>K. Hu, P. Ch. Ivanov, Z. Chen, P. Carpena, and H. E. Stanley, *Phys. Rev. E* **64**, 011114 (2001).
- <sup>23</sup>Z. Chen, P. Ch. Ivanov, K. Hu, and H. Stanley, *Phys. Rev. E* **65**, 041107 (2002).
- <sup>24</sup>H. E. Hurst, R. P. Black, and Y. M. Simaika, *Long-Term Storage: An Experimental Study* (Constable, London, 1965).
- <sup>25</sup>S. V. Buldyrev, A. L. Goldberger, S. Havlin, R. N. Mantegna, M. E. Matsuoka, C. K. Peng, M. Simons, and H. E. Stanley, *Phys. Rev. E* **51**, 5084 (1995).
- <sup>26</sup>B. Singha, A. Sarma, and J. Chutia, *Phys. Plasmas* **9**(2), 683 (2002).
- <sup>27</sup>S. Ghosh, P. K. Shaw, D. Saha, M. S. Janaki, and A. N. S. Iyengar, *Phys. Plasmas* **22**, 052304 (2015).
- <sup>28</sup>E. A. F. Ihelen, *Front. Physiol.* **3**(141), 141 (2012).
- <sup>29</sup>M. S. Movahed, G. R. Jafari, F. Ghasemi, S. Rahvar, and M. R. Tabar, *J. Stat. Mech.* P02003 (2006).